

# The value of simultaneous co-registration of $^{99m}\text{Tc}$ -MDP and $^{131}\text{I}$ Iodine in metastatic differentiated thyroid carcinoma

Magdy H. Kotb<sup>1</sup>, Walid Omar<sup>1</sup>, Tariq El-Maghraby<sup>2</sup>,  
Marwa El-Bedwihy<sup>1</sup>, Magdy El-Tawdy<sup>3</sup>, Hosna Mustafa<sup>2</sup>,  
Adil Al-Nahhas<sup>4</sup>

<sup>1</sup>Department of Nuclear Medicine, National Cancer Institute,  
Cairo University, Egypt

<sup>2</sup>Department of Nuclear Medicine, Cairo University, Egypt

<sup>3</sup>Department of Physics, Naser Oncology Centre, Cairo, Egypt

<sup>4</sup>Department of Nuclear Medicine, Hammersmith Hospital, London

[Received 28 IX 2007; Accepted 15 XI 2007]

## Abstract

**BACKGROUND:** The lack of anatomical details in standard  $^{131}\text{I}$  Iodine whole body scanning ( $^{131}\text{I}$  WBS) interferes with the proper localization of metastatic differentiated thyroid carcinoma (DTC) lesions. In addition, nearby or overlapping variable physiological distribution of  $^{131}\text{I}$  may affect the specificity of  $^{131}\text{I}$  uptake, giving indeterminate results. The aim of this study was to demonstrate the clinical usefulness of simultaneous co-registration of  $^{99m}\text{Tc}$  MDP bone scanning as an anatomical landmark with  $^{131}\text{I}$  scanning in the evaluation of metastatic DTC.

**MATERIAL AND METHODS:** Twenty-five patients (16 females and 9 males, mean age  $\pm$  SD =  $52 \pm 13$  years) with metastatic DTC (17 papillary, 8 follicular), were included. Whole body scanning using a  $256 \times 1024$  matrix and an 8 cm/min scan rate were obtained 48 hours after oral administration of 185–370 MBq  $^{131}\text{I}$  and 2 hours after IV administration of 185–370 MBq  $^{99m}\text{Tc}$  MDP using a dual head gamma camera equipped with high energy parallel hole collimators. Occasionally, additional simultaneous co-registration of localised detailed images was also performed using a  $256 \times 256$  ma-

trix size. The two planar images were fused with optional fusion of SPECT images.

The data from standard  $^{131}\text{I}$  scanning and fused  $^{131}\text{I}/^{99m}\text{Tc}$ -MDP scanning were separately assessed by two nuclear medicine physicians. Fusion images were considered to improve image interpretation in comparison with standard  $^{131}\text{I}$  scanning when they provided better localization of lesions.

**RESULTS:** All lesions in the present study were validated by radiological images and clinical follow up for at least 12 months. Forty-eight metastatic lesions were confirmed as follows: 2 in the skull, 10 in the neck, 20 in the thorax, 12 in the pelvic-abdominal region and 4 in the extremities. Standard  $^{131}\text{I}$  WBS showed 54 extra-thyroidal foci with 8 false positive lesions of which 2 were located in the scalp and 6 in the pelvic-abdominal region extra-skeleton (i.e. sensitivity 100%, specificity 86%). Out of the 48 validated lesions, 16 were indeterminately localized: 10 in the thorax (3 mediastinal nodal lesions, 5 vertebral lesions and 2 ribs) and 6 in the pelvic-abdominal region (2 upper sacral, 2 sacroiliac region and 2 ischial bone). Fusion images confirmed the precise localization of the pathological uptake in the validated 48 lesions (sensitivity 100%, specificity 100%). There were 2 (4%) indeterminate lesions in fused planar imaging that were clearly localized via fused SPECT images.

**CONCLUSIONS:** Fusion images using simultaneous co-registration of  $^{131}\text{I}$  and  $^{99m}\text{Tc}$  MDP scanning is a simple and feasible technique that improves the anatomically limited interpretation of scintigraphy using  $^{131}\text{I}$  alone in patients with metastatic differentiated thyroid carcinoma. The diagnostic advantage of this technique seems to be more apparent in the thoracic and pelvic-abdominal regions in contrast to the neck and extremities.

**Key words:** simultaneous Co-registration, differentiated thyroid carcinoma, Iodine-131 scan, technetium-99m-MDP bone scan

## Introduction

Differentiated thyroid cancer (DTC) is a common endocrine cancer and is reported as one of the most escalating human cancers [1]. DTC is an indolent tumour with a high chance of defini-

Correspondence to: Dr. Adil AL-Nahhas  
Department of Nuclear Medicine, Hammersmith Hospital  
Du Cane Road, London W12 0HS  
Tel: (+44) 208 383 4923, fax: (+44) 208 383 1700  
e-mail: aal-nahhas@hnt.org

tive cure due to its low metastatic potential. The high grade of differentiation and appropriate treatment with <sup>131</sup>Iodine therapy has lead to a long-term survival exceeding 90% [2]. A small proportion of patients (5–20%) with unfavourable prognostic risk factors will develop local or distant metastases, and when distant metastases are present, the overall survival rate declines to 40% after ten years. The metastatic sites are frequently the regional lymph nodes, followed in frequency by metastases to the lungs and the skeletal system [3–6]. The aim of post-surgical follow up is the early detection of metastases especially those that can lead to respiratory failure, airway obstruction and neurological complications that are considered major causes of death in DTC. Regular follow up with whole body iodine scanning and other functional and conventional imaging will improve the management and quality of life in a disease with known low intrinsic mortality rate [7].

Conventional imaging modalities used for follow up of DTC include ultrasonography for cervical lymph nodes, CT for lung metastases and MRI for brain lesions. However, <sup>131</sup>I whole-body scan (WBS) represents a cornerstone in routine follow up of these patients. The ability of thyroid malignant cells to trap and organify the iodine through the sodium-iodine symporter is the basis for the diagnostic and therapeutic use of <sup>131</sup>I [8]. The identification of abnormal areas of iodine uptake in the follow-up studies is the strongest evidence of metastases or recurrence. On the other hand, <sup>131</sup>I WBS has several limitations that interfere with its clinical value. The long half-life (8 days) and the sub-optimal physical characteristics (high gamma ray energy of 364 Kev), limit the administered dose significantly, leading to poor image quality. This leads to poor anatomical localisation of the abnormal foci seen on <sup>131</sup>I WBS. Moreover, <sup>131</sup>I is physiologically secreted in the salivary glands, stomach, gut and urinary tract leading to overlap and uncertainty in the identification of abnormal pathological metastatic foci. [9,10].

Proper anatomical localization in nuclear medicine imaging is an inherited problem that has encouraged multi-modality imaging with special fusion algorithms [11, 12]. Recently, hybrid scanners using SPECT or PET in combination with CT were introduced with great potential. Yet, the high technical demands and the high cost of these machines limit their availability. One particular problem regarding the modality of these hybrid scanners (SPECT/CT or PET/CT) in DTC patients is the need to avoid contrast agents for the CT part. Contrast agents (with high iodine content) will interfere with the future administration of radioiodine for diagnostic or therapeutic purposes for a variable period of time.

<sup>99m</sup>Tc-methylene diphosphonate (<sup>99m</sup>Tc-MDP) is commonly used for the detection of suspected skeletal metastases in patients with DTC. Bone scintigraphy represents an excellent method for visualizing the whole skeleton with great anatomical orientation. In a preliminary work, the usefulness of the addition of <sup>99m</sup>Tc-MDP bone scan to <sup>131</sup>I whole body scintigraphy for better anatomical localisation of bone metastases in DTC has been reported [13, 14]. However, such studies lack the technical details of these different scintigraphic techniques, particularly regarding the acquisition and processing of details.

The aim of the current work was to demonstrate the technical details of simultaneous acquisition of <sup>99m</sup>Tc-MDP bone scanning and <sup>131</sup>I whole body scanning, and secondly, to show the incremental clinical usefulness of combined co-registered images from

both <sup>99m</sup>Tc-MDP and <sup>131</sup>I for the accurate detection of local and distant metastases from DTC.

## Material and methods

The study was approved by the Committee Board of Radiotherapy and Nuclear Medicine department at the National Cancer Institute, Cairo. Informed consent was obtained from all patients and/or their relatives, with a complete description of the procedures. The work involved twenty-five patients with metastatic DTC (16 females and 9 males), average age  $52 \pm 13$  years. Histologically, there were 17 patients with papillary DTC and 8 patients with follicular DTC. All patients had thyroidectomy (near-total in 10 and total thyroidectomy in 15). Detailed patient characteristics are presented in Table 1. All cases had metastatic disease and the metastases were defined based on the appearances on neck ultrasound, CT, MRI and <sup>131</sup>I WBS. In addition, increased Thyroglobulin (Tg) levels, histological findings and evolution of the disease during subsequent follow up for at least 12 months were considered to confirm the presence of metastases.

### Scintigraphic procedures

The patients' TSH levels were assayed 4-6 weeks after thyroidectomy during which thyroid hormone replacement was withheld. The patients were considered legible for <sup>131</sup>I diagnostic WBS when TSH was  $> 30$  lu/ml. The patients were then given a dose of 5 mCi <sup>131</sup>I orally and imaged 48–72 hours later.

### Acquisition

The initial acquisition of <sup>131</sup>I WBS was performed using a large field of view gamma camera (E-cam Dual head-Siemens) fitted with a high-energy parallel-hole collimator. The photo-peak was 364 keV with symmetrical 20% window. The whole-body scan was done with a table speed of 6 cm/min. The next step on the imaging day was to intravenously inject the patient with 5 mCi of <sup>99m</sup>Tc-MDP and image after 2–3 hours.

### Fused <sup>99m</sup>Tc-MDP / <sup>131</sup>I-WBS scanning

The fusion scan acquisition started 2–3 hours post <sup>99m</sup>Tc-MDP injection using the same camera equipped with high-energy parallel-hole collimators. This acquisition was simultaneous using two different windows (15% window centred on 364 keV for <sup>131</sup>I and 15% window centred on 140 keV for <sup>99m</sup>Tc-MDP). The matrix resolution used in this fusion scan was  $256 \times 1024$  and the table speed was 8 cm/min. In some patients, additional spot views in fusion mode (matrix  $256 \times 256$ ), were acquired for more anatomical delineation. Optionally, SPECT images were obtained with dual-energy windows, 32 projections for each detector and a matrix resolution of  $64 \times 64$ .

**Table 1. Patient characteristics**

	PTC	FTC
Number (n)	17	8
Age: Years (mean $\pm$ SD)	48.8 $\pm$ 12	55 $\pm$ 15
Female: male	1.9:1	1.6:1
Thyroidectomy	17/17	8/8

PTC — papillary thyroid carcinoma; FTC — follicular thyroid carcinoma; SD — standard deviation

### Data processing and image fusion

The planar data provide two simultaneously co-registered separate images with two different count intensity scales. Processing entails successful fusion of these two images with preservation of the data from the two scale producing single scale image that maintain high target to background (T/B) ratio. This is obtained by tuning the intensity of  $^{131}\text{I}$  images using variable multiplication factor (K) for  $^{131}\text{I}$  matrix to approximate the count intensity of the  $^{99\text{m}}\text{Tc}$ -MDP image. This count-intensity tuned image will be summed to the bone-scan image providing a single-scale image with satisfactory T/B ratio.

### Images analysis and interpretation

Two experienced nuclear medicine physicians were responsible for visual interpretation of the images on a lesion-by-lesion basis for detection of metastases in lymph nodes, lungs, bones and other regions. The findings were defined as positive or negative based on consensus.

The  $^{131}\text{I}$  WBS and fusion scintigraphy were interpreted independently of each other, then all the images were re-evaluated based on the fusion images including knowledge of the results of the  $^{131}\text{I}$ -WBS scintigraphy.

The usefulness of fusion scintigraphy was assessed based on whether:

- fusion scintigraphy provided additional anatomical information that solves the problem of indeterminate lesions on  $^{131}\text{I}$ -WBS;
- fusion scintigraphy provided additional anatomical information that changed the previous staging of the patient, based on the  $^{131}\text{I}$ -WBS alone;
- fusion SPECT scintigraphy provided more detailed information than the planar fusion scintigraphy.

## Results

The total number of definite metastases was 48 lesions. The highest distribution of metastatic lesions was in the lungs, bones or both, with a frequency of 10 (21%), 8 (16%) and 22 (46%),

respectively. Nodal metastases were found in 8 cases (16%). Metastatic lesions were 27/48 (56%) from papillary DTC and 21/48 (44%) from follicular DTC. The details of the distribution and frequency of these metastatic lesions are shown in Table 2.

Regional anatomical distribution of metastatic lesions showed that the highest number 20/48 (42%) was present in the thoracic region, and the lowest was in the head region 2/48 (4%). Variable anatomical distribution was seen in the neck, extremities and pelvi-abdominal areas, as shown in Table 3.

### $^{131}\text{I}$ whole body scintigraphy ( $^{131}\text{I}$ -WBS)

There were 56 areas of focal uptake on  $^{131}\text{I}$  WBS. All metastatic lesions showed positive focal uptake on the  $^{131}\text{I}$  Whole Body Scan (WBS) with a sensitivity of 100%. However, an additional eight false-positive focal areas were seen reducing the specificity to 86%.

Findings in  $^{131}\text{I}$ -WBS were divided into two groups. Group A, Positive  $^{131}\text{I}$  metastatic lesions that are well localized anatomically, which included 32 lesions (67%). Group B, are the  $^{131}\text{I}$  metastatic lesions that are anatomically indeterminate, which included 16/48 lesions (33%) and included 10 lesions in the thorax and 6 in the pelvi-abdominal region.

### $^{131}\text{I}$ -WBS and $^{99\text{m}}\text{Tc}$ -MDP bone scan fusion scintigraphy

As indicated in Table 4, the addition of bone scintigraphy and the resultant fusion ( $^{131}\text{I}$  and MDP) scintigraphy correctly identified 48 metastatic lesions out of the 56  $^{131}\text{I}$  positive lesions. The remaining eight  $^{131}\text{I}$  focal areas that were seen in  $^{131}\text{I}$ -WBS but not anatomically defined by  $^{99\text{m}}\text{Tc}$ -MDP bone scan were located in the scalp, large bowel and pelvic regions. Accordingly, these were considered false positive findings by  $^{131}\text{I}$  WBS. The remaining 48 lesions were considered true positives, and, therefore, the specificity of the fusion scan was 100%.

**In group A**, fusion scintigraphy confirmed the  $^{131}\text{I}$  findings with concordant agreement between both  $^{131}\text{I}$  and fusion scan of 100%.

**In group B**, out of 16 anatomically indeterminate lesions, planar fusion scans localized 14 lesions accurately (87%). The other two

**Table 2. Sites of metastases from DTC**

Site of metastases (n = number)	Overall (n = 48)	PTC (n = 27)	FTC (n = 21)
Nodal	8	6	2
Lungs	10	6	4
Bones	8	3	5
Lungs and bones	22	12	10

PTC — papillary thyroid carcinoma; FTC — follicular thyroid carcinoma

**Table 3. Distribution of metastases by region**

Region of metastases	Overall (n = 48)	PTC (n = 27)	FTC (n = 21)
Skull	2	1	1
Neck	10	7	3
Thorax	20	12	8
Pelvi-abdominal	12	6	6
Extremities	4	1	3

PTC — papillary thyroid carcinoma; FTC — follicular thyroid carcinoma

**Table 3. Distribution of metastases by region**

Region of metastases	Overall (n = 48)	PTC (n = 27)	FTC (n = 21)
Skull	2	1	1
Neck	10	7	3
Thorax	20	12	8
Pelvi-abdominal	12	6	6
Extremities	4	1	3

PTC — papillary thyroid carcinoma; FTC — follicular thyroid carcinoma

**Table 4. Findings of standard I-131 and fused I-131 / MDP bone scans**

	Standard I-131 (n = 56)	Fused I-131/ MDP scans (n = 48)
TP	48	48
FP	8	0
Sensitivity	100%	100%
Specificity	86%	100%

TP — true positive, FP — false positive, n — number of patients

lesions were clearly identified by SPECT of fused <sup>131</sup>I and MDP scintigraphy and were in the thorax and pelvi-abdominal regions. Table 5 shows the effect of fused planar <sup>131</sup>I/<sup>99m</sup>Tc-MDP scans in the identification of indeterminate lesions by standard <sup>131</sup>I WBS.

### Change in management

Change in management of patients occurred in 3/8 patients who had false-positive findings by <sup>131</sup>I-WBS alone. Of those three patients, one had false positive scalp lesion, and the other 2 patients had false-positive colonic activity. Those three patients were down-staged from distant metastases to local metastases, as they already had involved cervical lymph node metastases.

### Discussion

The early detection of recurrence and/or metastases is essential for further management in DTC. Following thyroidectomy and post surgical ablation, periodic follow up with <sup>131</sup>I WBS remains a reliable test for the management of DTC patients. The presence of pathological foci of <sup>131</sup>I accumulation in the neck, chest or skeletal system is strong evidence for recurrence or metastases [13, 15–17]. However, several inherent limitations remain challenging and influence the reliability of this technique. One notable limitation is

the physiological secretion and excretion of <sup>131</sup>I from the salivary glands, stomach, bowel and urinary system, which are considered the most common causes of false-positive results. Moreover, accumulation of <sup>131</sup>I in some inflammatory conditions, especially in bowel and lungs with variable rate of turnover, is not uncommon. This may provide a potential source of error when misinterpreted as positive for DTC. The limited anatomical information from this functional technique has a major impact in this misinterpretation and in many instances provides indeterminate results [18, 19].

Recently the effectiveness of simultaneous dual isotope co-registration using a combination of <sup>99m</sup>Tc-MDP diphosphonate and <sup>131</sup>I scanning for localization of metastases of DTC has been reported. <sup>99m</sup>Tc-MDP scans can provide an internal anatomical landmark that, when fused with <sup>131</sup>I scanning, can help in the localization of iodine-avid foci. However, these reports did not show the technical details of the fusion process [20, 14].

The aim of this technique is to fuse two simultaneously co-registered images with two different intensity scales yielding a single scale intensity image that preserves the data of the two scales with a high T/B ratio. There are several factors that should be considered with this technique, including: using single energy line isotopes, adequate energy gap between the two energy windows to limit cross talking, proper selection of collimator (use a higher energy collimator to reduce penetration of collimator septa), use of high-speed detector electronics (i.e. fast response time to enhance count efficiency) and finally consider the quantity of used radio-activity for each isotope to create a balance in the count collected for each study.

Based on the above-mentioned considerations, we used a high-energy collimator and limited the injected dose of <sup>99</sup>Tc-MDP to 185–370 MBq, as the bone scanning was considered only as an anatomical landmark. This may yield a sub-optimal bone scan quality but avoids acquiring too much count from the scale of bone display, which may obscure the iodine-avid lesions and fa-

**Table 5. Effect of fused planar I-131/MDP scans in identification of indeterminate lesions**

	Indeterminate lesions Number of lesions		Effect of planar fusion scan Decrease with I-131/MDP (%)
	I-131 (n = 16)	I-131/MDP (n = 2)	
Thorax	10	1	90%
Pelvic-abdominal	6	1	83%
Skull, neck	0	0	0%
Extremities	16/48	2/48	
Total	33%	4%	29%

n — number of patients. Fused SPECT images clarify the 2 indeterminate lesions of fused planar images

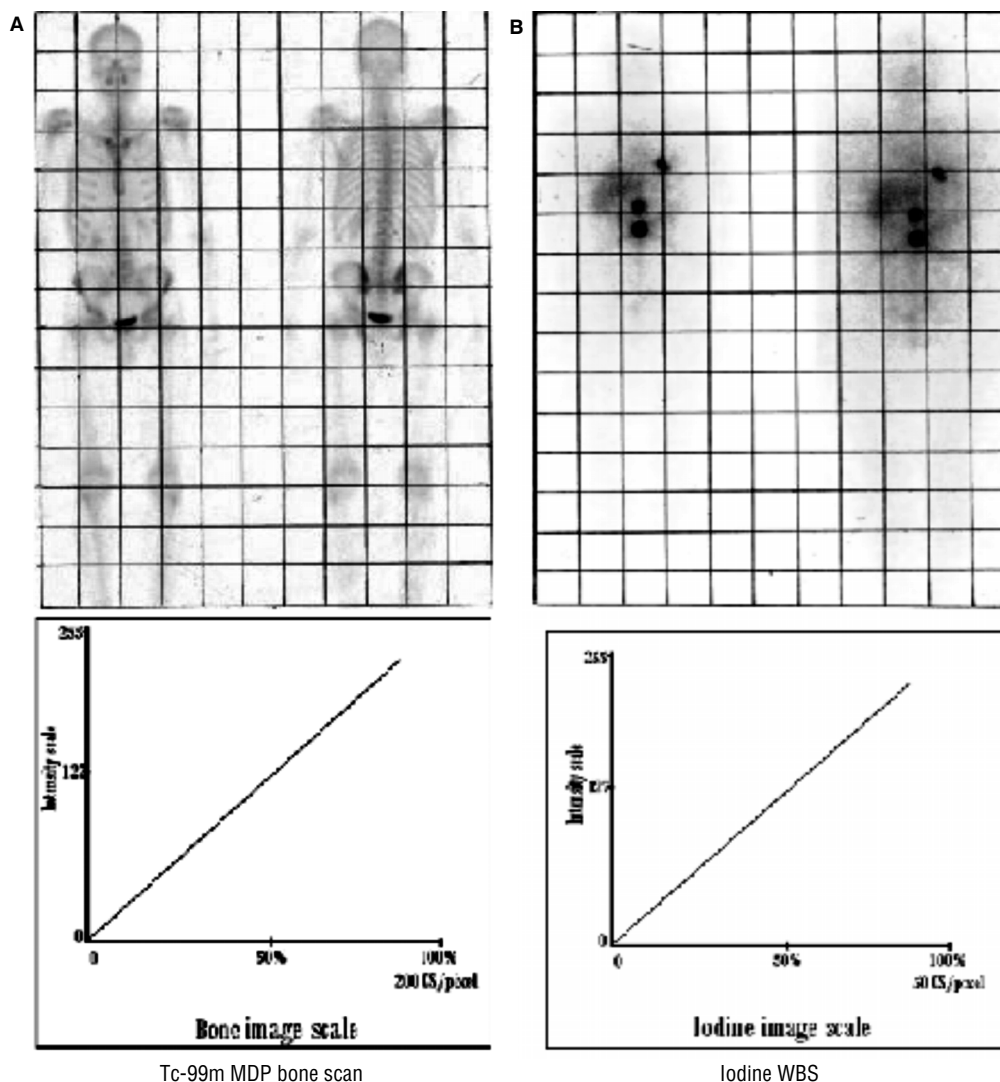


**Figure 1.** The difference in intensity scales and count per pixel for  $^{99m}\text{Tc}$ -MDP and  $^{131}\text{I}$  scans. **A.** Figure shows the difference in count intensity between bone and iodine scan intensity; **B.** Figure shows the difference between count per pixel for iodine and bone scale. Image manipulation entails the use of variable multiplication factor (K) for I-131 image followed by summation of iodine and bone scan images producing fused image with single intensity scale.

cilitates the process of fusion with a satisfactory T/B ratio. Therefore, the sensitivity of  $^{99m}\text{Tc}$ -MDP bone scan in the detection of DTC was relatively underestimated (40%) compared to other reports (60%) [21, 20].

Tuning between the two images with different count intensity scales was done through the use of variable multiplication factor (K) for  $^{131}\text{I}$  image matrix before matrix summation, which yields a satisfactory fused image with a single intensity scale and provides a reasonable T/B ratio (Figure 1). This process of matrix multiplication and image summation is not applicable for fused SPECT images because separation between the acquired SPECT data in two different scales, one for each isotope, is not possible. However, the relatively limited injected dose of  $^{99m}\text{Tc}$ -MDP and collection of data through 360 degree around the object create a reasonable balance between T/B ratio after reconstruction (Figures 2, 3).

DTC has been reported to be 2–4 times more frequent in females than in males although the rate is lower for patients with distant metastases [22]. In our study, where all patients had metastases of DTC, the female: male ratio was 1.9:1 for PTC and

1.6:1 for FTC, further supporting the higher relative risk of distant metastases among males [23]. Similar to other results [24, 6, 25], in the present study FTC was more frequent in males and had a higher rate of metastatic potential compared to PTC (21 metastatic lesions/8 FTC patients compared to 27 metastatic lesions for 17 PTC patients). The distribution by sites for distant metastases corresponded to the results of other studies [3, 4].

In practice, indeterminate localization of iodine-avid foci in  $^{131}\text{I}$  WBS requires complementary morphological imaging modalities (U/S, CT and/or MRI) for clarification. While these techniques provide excellent anatomical information compared to functional nuclear medicine imaging, they have some diagnostic limitations. These limitation include the inability to detect disease in lymph nodes (LNs) that are not or are only slightly enlarged (sub-centimetre nodes), differentiation of scar tissue or fibrosis from local recurrence, and the limited ability in monitoring the response to therapy. Moreover, the difference in the mechanisms of assessing malignancy with functional vs. anatomical imaging creates some discrepancy in their results. Another limiting factor is the

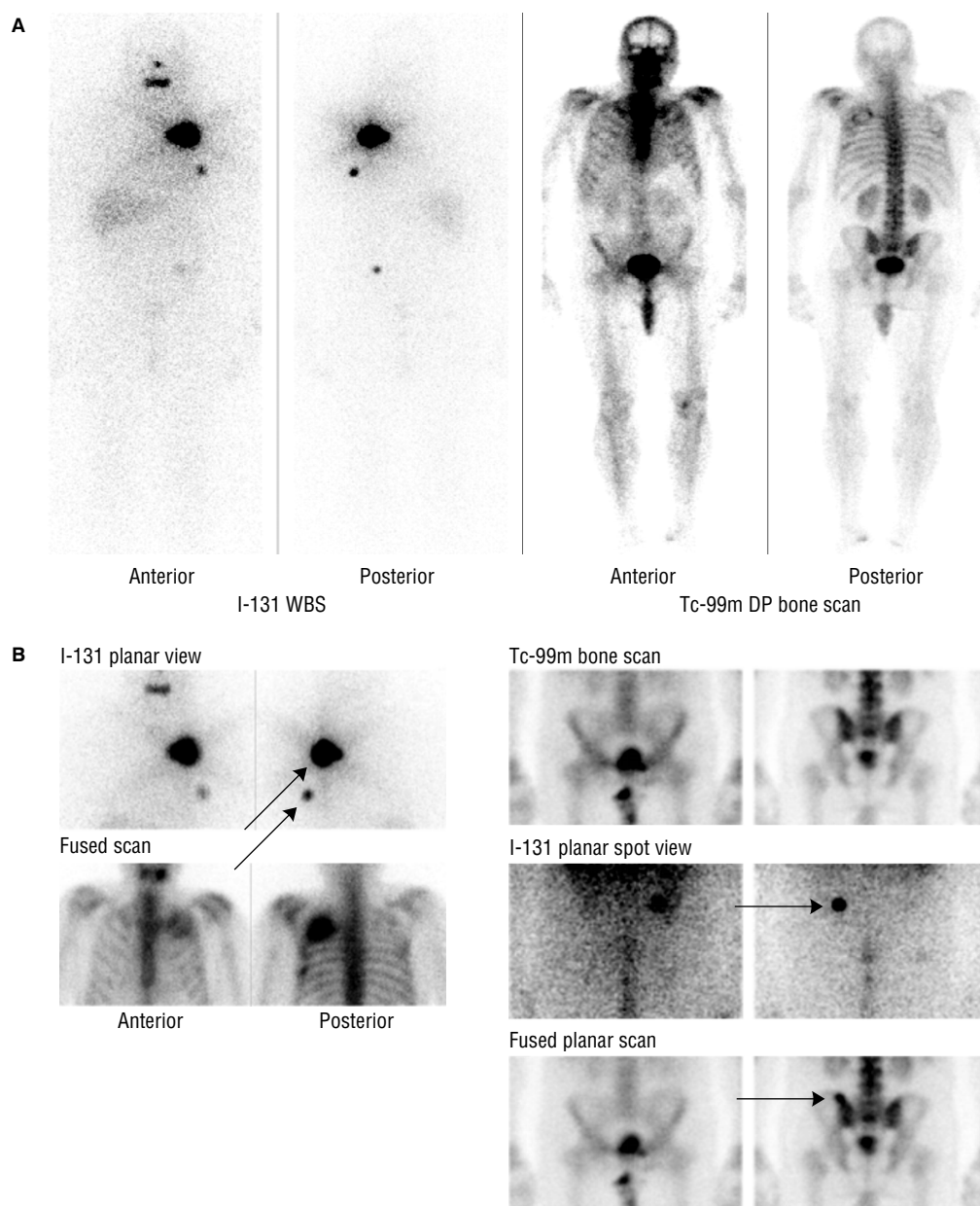


**Figure 2A.**  $^{131}\text{I}$  WBS and bone performed for 48-year-old male patient with metastatic disease before fusion FCT. Out of the three who demonstrated hot foci in  $^{131}\text{I}$ , two were indeterminately localized, one was located in the thoracic region and the other was located in the pelvic region. **B.** Figure shows multi-spot anterior and posterior planar views before and after fusion. The fused planar images clearly identify the location of hot foci in left ribs posteriorly as well as left ala close to tip of sacro-iliac region.

use of CT with contrast, which limits further radioiodine administration [14, 19, 26, 27].

The clinical usefulness of using a combination of  $^{99m}\text{Tc}$ -MDP and  $^{131}\text{I}$  scanning for localization of metastases from DTC has been previously described by Johann Schoenberger and colleagues [14]. They gained additional information in 16 of 21 patients because the presence of osseous structures from bone scintigraphy facilitates the correct diagnosis of the lymph node involved; the identification of distant metastases and delineation of residual thyroid tissue from lymph node metastases after thyroidectomy. In the present study, simultaneous co-registered fused  $^{131}\text{I}/^{99m}\text{Tc}$ -MDP scanning was able to depict eight false positive iodine-avid foci in standard  $^{131}\text{I}$  WBS. Most of these foci were linked to

persistent focal colonic activity located in the pelvic-abdominal region. Therefore, the specificity of the simultaneous co-registered combined  $^{131}\text{I}/^{99m}\text{Tc}$ -MDP was 100% compared to 86% for standard  $^{131}\text{I}$ . This resulted in disease down-staging in three patients and a change in the strategy of therapy.

The present study shows concordant agreement between both standard  $^{131}\text{I}$  and fusion planar scans in 32 out of 48 (67%) lesions. Concordant results were higher in the skull, neck and extremities compared to the thoracic and pelvic-abdominal regions. On the other hand, the planar fused scans provided additional anatomical information in 87% of indeterminate lesions by outlining bones. Fused SPECT images improved the detectability of two indeterminate lesions in fused planar images by providing

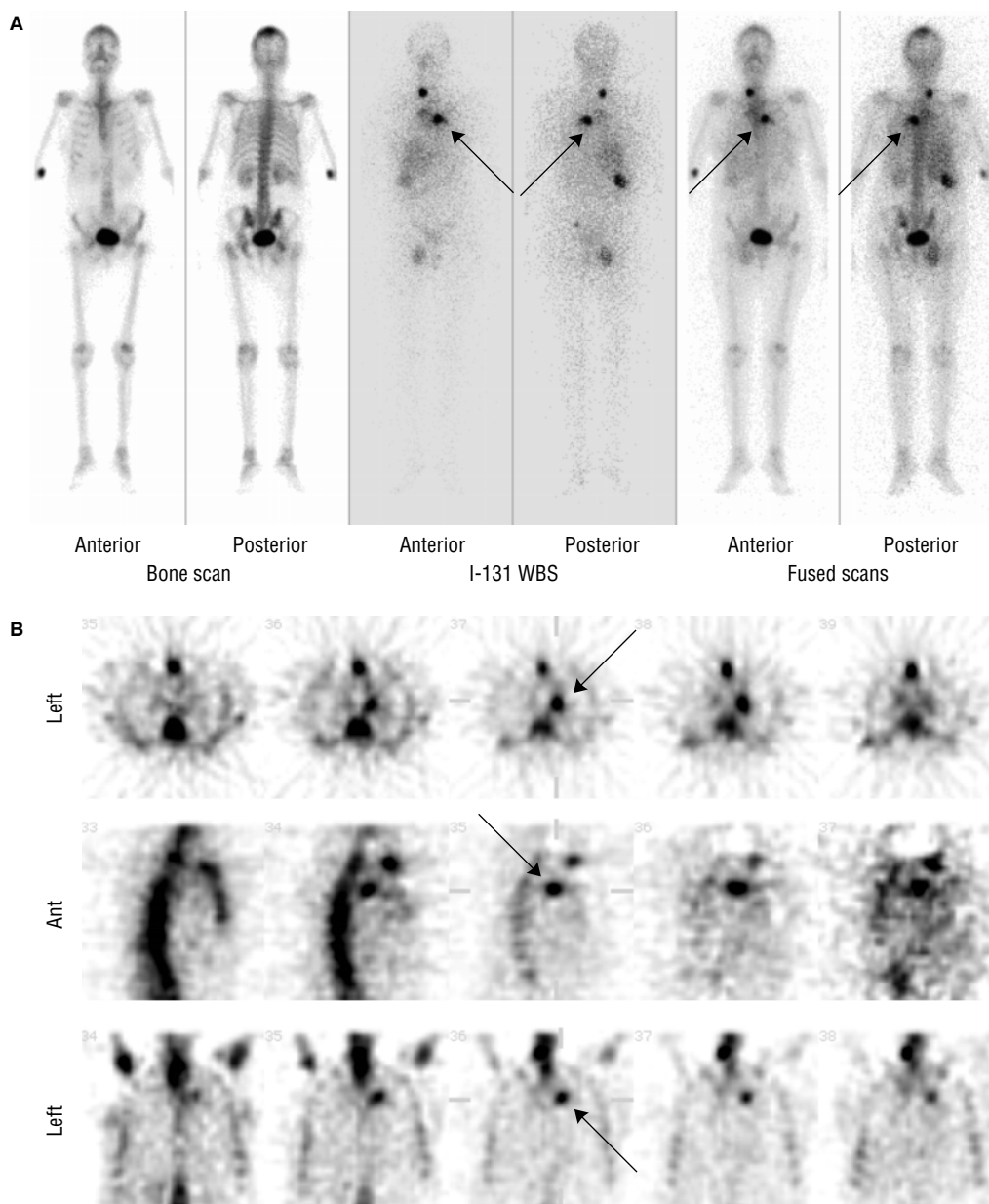


**Figure 3A.**  $^{99m}\text{Tc}$ -MDP bone scan (left column), standard  $^{131}\text{I}$  WBS (middle column) and fused scans (right column) in a female patient with multiple metastatic hot foci. The planar fused image cannot clarify totally the indicated intra-thoracic lesion because of overlapping structures. **B.** Reconstructed transverse, sagittal and coronal slices for thoracic region for the same patient showing the hot foci to be nodal mediastinal lesion.

more anatomical information with better contrast enhancement and solved the problem of overlapping structures.

We have shown, in selected cases, that fusion scintigraphy using the mentioned simultaneous co-registration of  $^{131}\text{I}/^{99m}\text{Tc}$ -MDP method is helpful in the localization of pathological tracer accumulation through delineation of intra- and extra-osseous foci. Moreover, simultaneous acquisition of both nuclides excludes patient motion artefact and facilitates fusion processing and manipulation.

Recently, newly developed machines that combined CT and a gamma camera (SPECT/CT) were introduced and showed great potential. The combination of functional imaging with the anatomical details of multi-slice CT represents the best solution in cases involving metastatic DTC. However, the high cost of this machine

and limited availability interferes with the wide distribution of this advanced technology. In addition, contrast related technical problems remain challenging, particularly in DTC patients, as they interfere with further administration of radioiodine in those patients. Therefore, fused scintigraphy offers an effective existing alternative technique that is available in many nuclear medicine departments.

## Conclusions

Fusion imaging using simultaneous co-registration of  $^{131}\text{I}$  and  $^{99m}\text{Tc}$  MDP scanning is a simple and feasible technique that improves the anatomically limited interpretation of scintigraphy using  $^{131}\text{I}$  alone, in patients with metastatic DTC. Simultaneous exploration of osseous structures and areas of high  $^{131}\text{I}$  uptake in

fused scintigraphy allow clear delineation of osseous and extra-osseous foci. Moreover, the added anatomical information from fused scans significantly reduces false positive and indeterminate results. The diagnostic advantage of this technique seems to be more apparent in the thoracic and pelvi-abdominal regions than in the neck and extremities.

## References

1. Samaan NA, Schultz PN, Hickey RC et al. The results of various modalities of treatment of well differentiated thyroid carcinomas: a retrospective review of 1599 patients. *J Clin Endocrinol Metab* 1992; 75: 714–720.
2. Zettinig G, Fueger BJ, Passler C et al. Long-term follow-up of patients with bone metastases from differentiated thyroid carcinoma — surgery or conventional therapy? *Clin Endocrinol (Oxf)* 2002; 56: 377–382.
3. Schlumberger M, Tubiana M, De Vathaire F, Hill C, Gardet P, Travagli JP. Long-term results of treatment of 283 patients with lung and bone metastases from differentiated thyroid carcinoma. *J Clin Endocrinol Metab* 1986; 63: 960–967.
4. Ruegamer JJ, Hay ID, Bergstrahl EJ, Ryan JJ, Offord KP, Gorman CA. Distant metastases in differentiated thyroid carcinoma: a multivariate analysis of prognostic variables. *J Clin Endocrinol Metab* 1988; 67: 501–508.
5. Hoie J, Stenwig AE, Kullmann G, Lindegaard M. Distant metastases in papillary thyroid cancer. A review of 91 patients. *Cancer* 1988; 61: 1–6.
6. Mizukami Y, Michigishi T, Nonomura A et al. Distant metastases in differentiated thyroid carcinomas: a clinical and pathologic study. *Hum Pathol* 1990; 21: 283–290.
7. Kitamura Y, Shimizu K, Nagahama M et al. Immediate causes of death in thyroid carcinoma: clinicopathological analysis of 161 fatal cases. *J Clin Endocrinol Metab* 1999; 84: 4043–4049.
8. Spitzweg C, Morris JC. Sodium iodide symporter (NIS) and thyroid hormones (Athens). 2002; 1: 22–34.
9. Freitas JE, Gross MD, Ripley S, Shapiro B. Radionuclide diagnosis and therapy of thyroid cancer: current status report. *Semin Nucl Med* 1985; 15: 106–131.
10. Shapiro B, Rufini V, Jarwan A et al. Artifacts, anatomical and physiological variants, and unrelated diseases that might cause false-positive whole-body <sup>131</sup>I scans in patients with thyroid cancer. *Semin Nucl Med* 2000; 30: 115–132.
11. Lang TF, Hasegawa BH, Liew SC et al. Description of a prototype emission-transmission computed tomography imaging system. *J Nucl Med* 1992; 33: 1881–1887.
12. Beyer T, Townsend DW, Brun T et al. A combined PET/CT scanner for clinical oncology. *J Nucl Med* 2000; 41: 1369–1379.
13. Tenenbaum F, Schlumberger M, Bonnin F et al. Usefulness of technetium-99m hydroxymethylene diphosphonate scans in localizing bone metastases of differentiated thyroid carcinoma. *Eur J Nucl Med* 1993; 20: 1168–1174.
14. Schoenberger J, Fuchs E, Fertig V, Szikszai A, Maenner P, Eilles C. Clinical value of planar and tomographic dual-isotope scintigraphy using <sup>99m</sup>Tc-methylene diphosphonate and <sup>131</sup>I in patients with thyroid cancer. *Nucl Med Commun* 2006; 27: 865–871.
15. Pacini F. Follow-up of differentiated thyroid cancer. *Eur J Nucl Med Mol Imag* 2002; 29 Suppl 2: S492–S496.
16. Kinder BK. Well differentiated thyroid cancer. *Curr Opin Oncol* 2003; 15: 71–77.
17. Pacini F, Schlumberger M, Dralle H, Elisei R, Smit JW, Wiersinga W. European Thyroid Cancer Taskforce. European consensus for the management of patients with differentiated thyroid carcinoma of the follicular epithelium. *Eur J Endocrinol* 2006; 154: 787–803.
18. Shapiro B, Rufini V, Jarwan A et al. Artifacts, anatomical and physiological variants, and unrelated diseases that might cause false-positive whole-body <sup>131</sup>I scans in patients with thyroid cancer. *Semin Nucl Med* 2000; 30: 115–132.
19. Yamamoto Y, Nishiyama Y, Monden T, Matsumura Y, Satoh K, Ohkawa M. Clinical usefulness of fusion of <sup>131</sup>I SPECT and CT images in patients with differentiated thyroid carcinoma. *J Nucl Med* 2003; 44: 1905–1910.
20. Ceccarelli C, Bianchi F, Trippi D et al. Location of functioning metastases from differentiated thyroid carcinoma by simultaneous double isotope acquisition of I-131 whole body scan and bone scan. *J Endocrinol Invest* 2004; 27: 866–869.
21. Zettinig G, Leitha T, Niederle B et al. FDG positron emission tomographic, radioiodine, and MIBI imaging in a patient with poorly differentiated insular thyroid carcinoma. *Clin Nucl Med* 2001; 26: 599–601.
22. Mazzaferri EL, Kloos RT. Clinical review 128: Current approaches to primary therapy for papillary and follicular thyroid cancer. *J Clin Endocrinol Metab* 2001; 86: 1447–1463.
23. Shoup M, Stojadinovic A, Nissan A, Ghossein RA, Freedman S, Brennan MF et al. Prognostic indicators of outcomes in patients with distant metastases from differentiated thyroid carcinoma. *J Am Coll Surg* 2003; 197: 191–197.
24. Wood WJ Jr, Singletary SE, Hickey RC. Current results of treatment for distant metastatic well-differentiated thyroid carcinoma. *Arch Surg* 1989; 124: 1374–1377.
25. Schlumberger MJ. Papillary and follicular thyroid carcinoma. *N Engl J Med* 1998; 338: 297–306.
26. van den Brekel MW, Stel HV et al. Cervical lymph node metastasis: assessment of radiologic criteria. *Radiology* 1990; 177: 379–84.
27. Alam MS, Takeuchi R, Kasagi K et al. Value of combined technetium-99m hydroxymethylene diphosphonate and thallium-201 imaging in detecting bone metastases from thyroid carcinoma. *Thyroid* 1997; 7: 705–712.